

On the Separation of Enantiomers by Drift Tube Ion Mobility Spectrometry

Roberto Fernández-Maestre,^{1,2} and Markus Doerr³

¹ Departamento de Química, Campus de San Pablo, Universidad de Cartagena, Cartagena, Colombia.

² National Research Nuclear University MEPhI (Moscow Engineering Physics Institute), Kashirskoe sh. 31, Moscow, 115409, Russia. *rfernandezm@unicartagena.edu.co

³ Universidad Industrial de Santander, Cra 27 Calle 9, Bucaramanga, Colombia. mhodoerr@uis.edu.co

Supporting Information

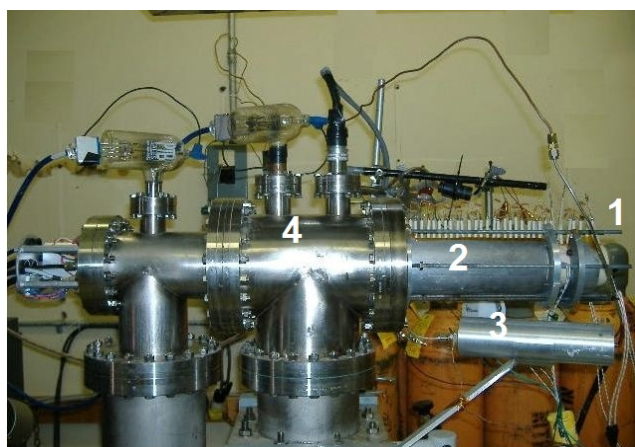


Figure S1. Photograph of the electrospray ionization-atmospheric pressure ion mobility-mass spectrometer. 1. Desolvation region 2. Drift region 3. Buffer gas heater 4. Mass spectrometer

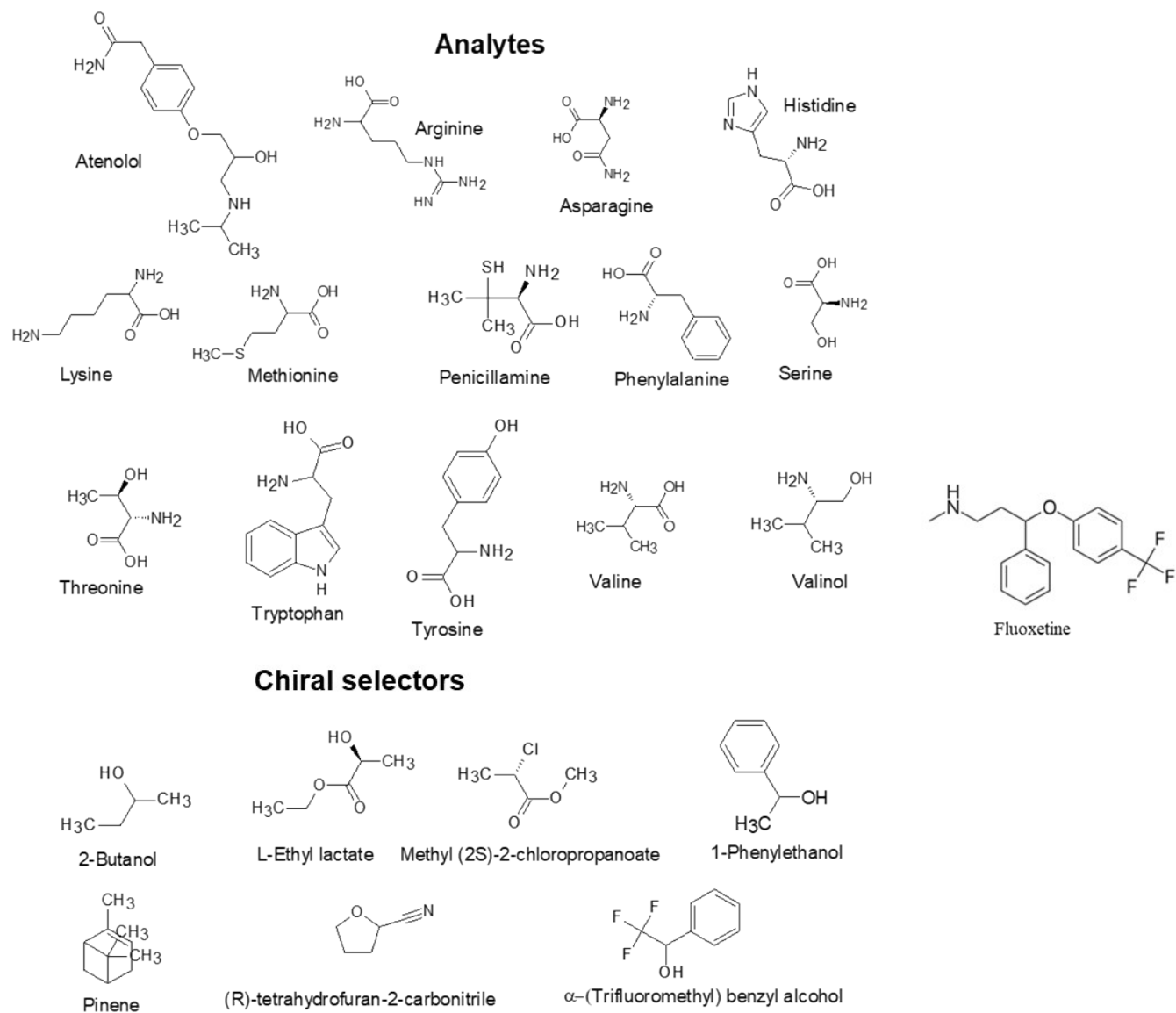


Figure S2. Chiral analytes and chiral selectors for enantiomer separation experiments

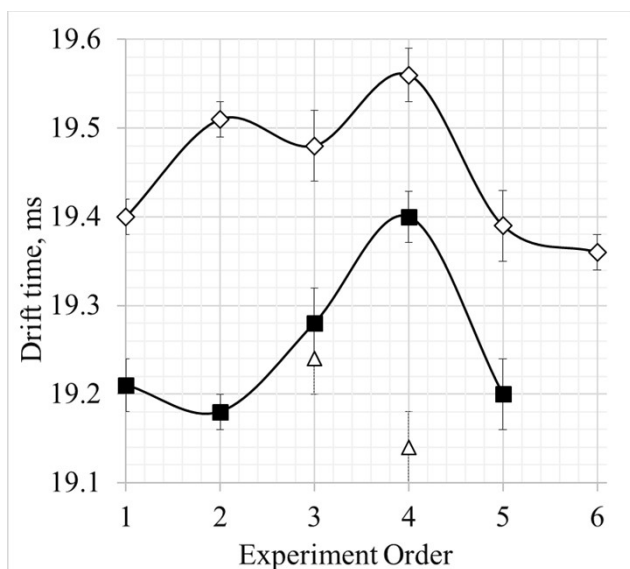


Figure S3. Stability of the mobilities of valine enantiomers with time. Drift times of valine enantiomers over an 8-hr period using 0.69 mmol m^{-3} of (S)-2-butanol chiral selector. Solutions of D-valine (\odot), L-valine (\diamond) and racemic mixtures of valine (Δ) at a $943\text{-}\mu\text{M}$ concentration were analyzed at 150°C . The racemic mixtures yielded only one peak. Data were obtained in the SIM-MS mode selecting the mass of protonated valine (Table S4). The analyses were made by switching between the D and L enantiomers of valine. The drift times variation was caused mainly by atmospheric pressure drift. The drift times of the enantiomers showed a small difference of $\sim 0.15\text{-}0.3$ ms between the enantiomers, too small to observe their individual peaks in a mixture according to the resolving power of the mobility spectrometer (~ 100). Additionally, the racemic mixtures yielded only one peak (experiments 2 and 3 in this figure). However, in several other experiments this behavior was not observed (Table 1).

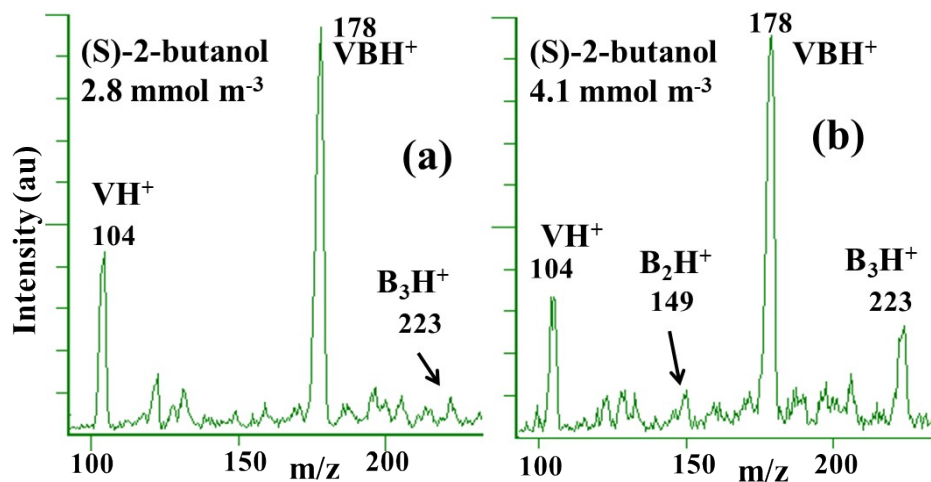
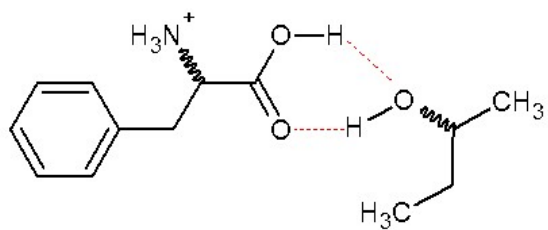
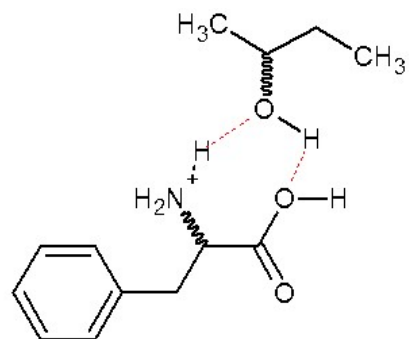


Figure S4. Increasing formation of clusters at high (S)-2-butanol concentrations. MS spectra of a 943- μ M solution of D-valinol (V) at 150 °C when the concentration of (S)-2-butanol (B) in the buffer gas increased from (a) 2.8 mmol m^{-3} to (b) 4.1 mmol m^{-3} . Other experimental conditions were those of Figure S3. When the (S)-2-butanol concentration increased, the intensity of VH^+ decreased with respect to VBH^+ because this cluster increased, as expected if the cluster was formed from protonated valinol, VH^+ . This figure also illustrates the expected increase in intensity of the peaks of the dimer (B_2H^+ , m/z 149) and trimer (B_3H^+ , m/z 223) of (S)-2-butanol when the chiral selector concentration increased.



Interaction with the carboxylic group



Interaction with the amine group

Figure S5. Phenylalanine:2-butanol interaction

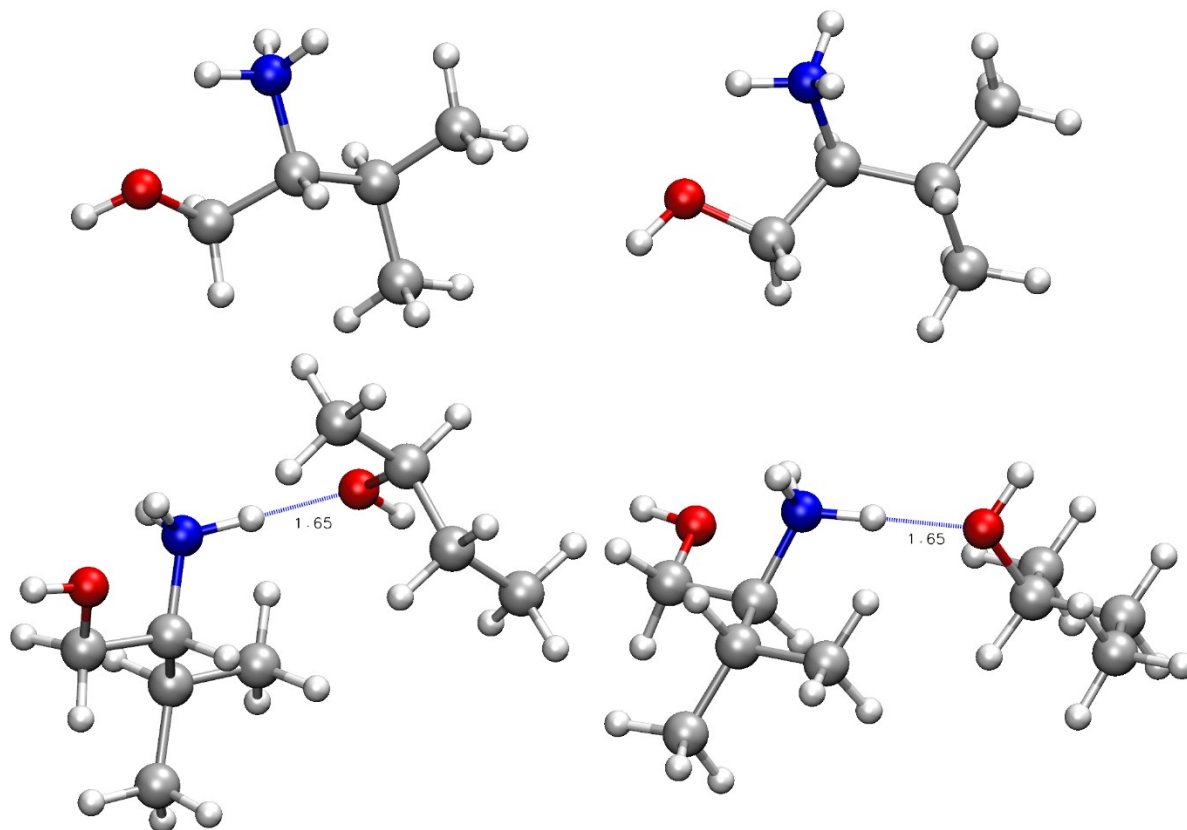


Figure S6. Isolated chiral valinol cations (above) and their lowest energy structures complexes with 2-butanol (below). The bond lengths and angles of all hydrogen bonds are very similar, consistent with the similar binding energies. All figures were created with VMD. Numbers indicate bond lengths (in Å) and angles of the hydrogen bonds (in °).

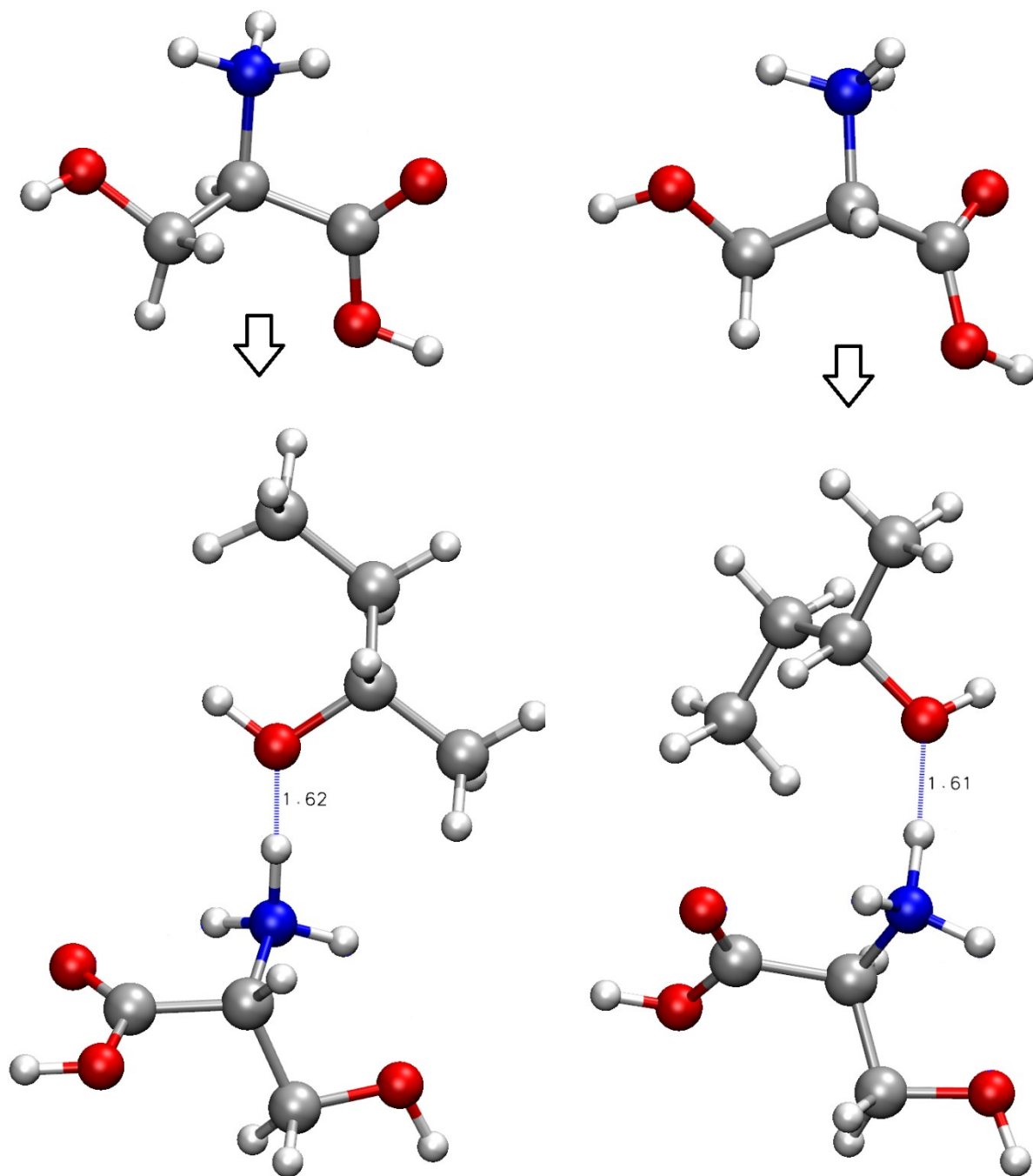


Figure S7. Isolated chiral serine cations (above) and their lowest energy structures complexes with 2-butanol (below). The bond lengths and angles of all hydrogen bonds are very similar, consistent with the similar binding energies. All figures were created with VMD. Numbers indicate bond lengths (in Å) and angles of the hydrogen bonds (in °).

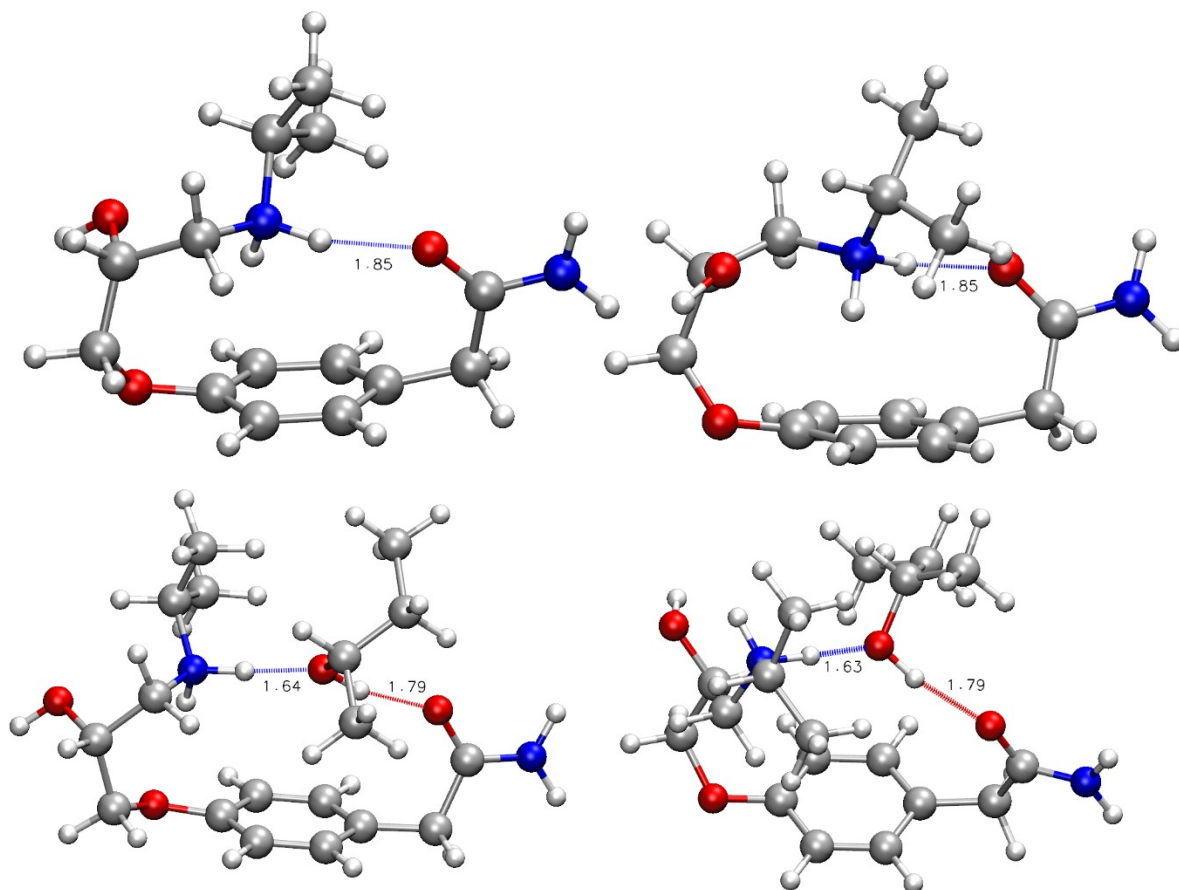


Figure S8. Isolated chiral atenolol cations (above) and their lowest energy structures complexes with 2-butanol (below). There is steric hindrance on the charge for the attachment of 2-butanol to protonated atenolol because there is an intramolecular bond between the amine groups as reported before.³⁴⁻³⁷ This bond delocalizes the charge weakening the ion-SR interactions. The steric hindrance restricts the possible orientations of the butanol molecule in the complex. In the publication, we restrict the analysis to the structures with the lowest free energy. However, we also found structures with somewhat higher free energies, which are also expected to be populated at the experimental temperature. In these structures, butanol adopts different orientations which all preserve the same H-bonding pattern. This shows that there is some rotational flexibility around the two H-bonds. The bond lengths and angles of all hydrogen bonds are very similar, consistent with the similar binding energies. All figures were created with VMD. Numbers indicate bond lengths (in Å) and angles of the hydrogen bonds (in °).

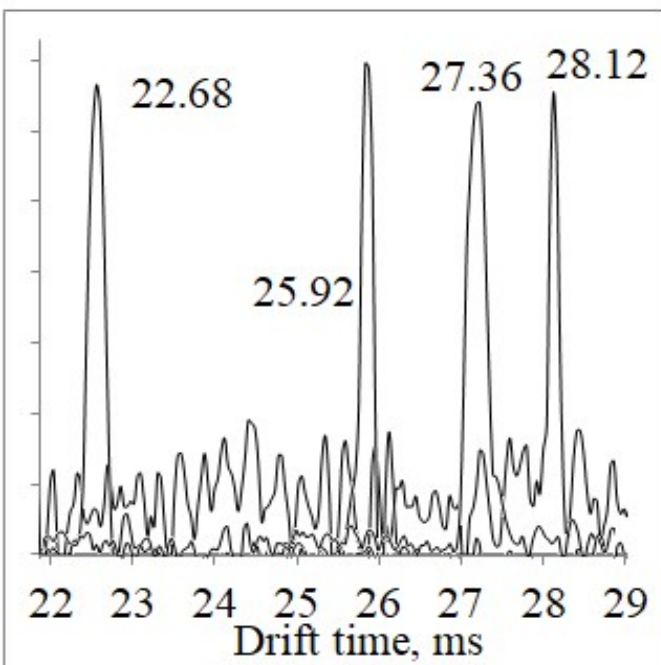


Figure S9. Superimposed IMS spectra of a racemic mixture of methionine when the (R)-1-phenylethanol chiral selector flow rate was increased from 0 to 60 $\mu\text{l hr}^{-1}$. The drift time increased from 22.68 ms at 0 $\mu\text{l hr}^{-1}$ to 28.12 ms at 60 $\mu\text{l hr}^{-1}$.

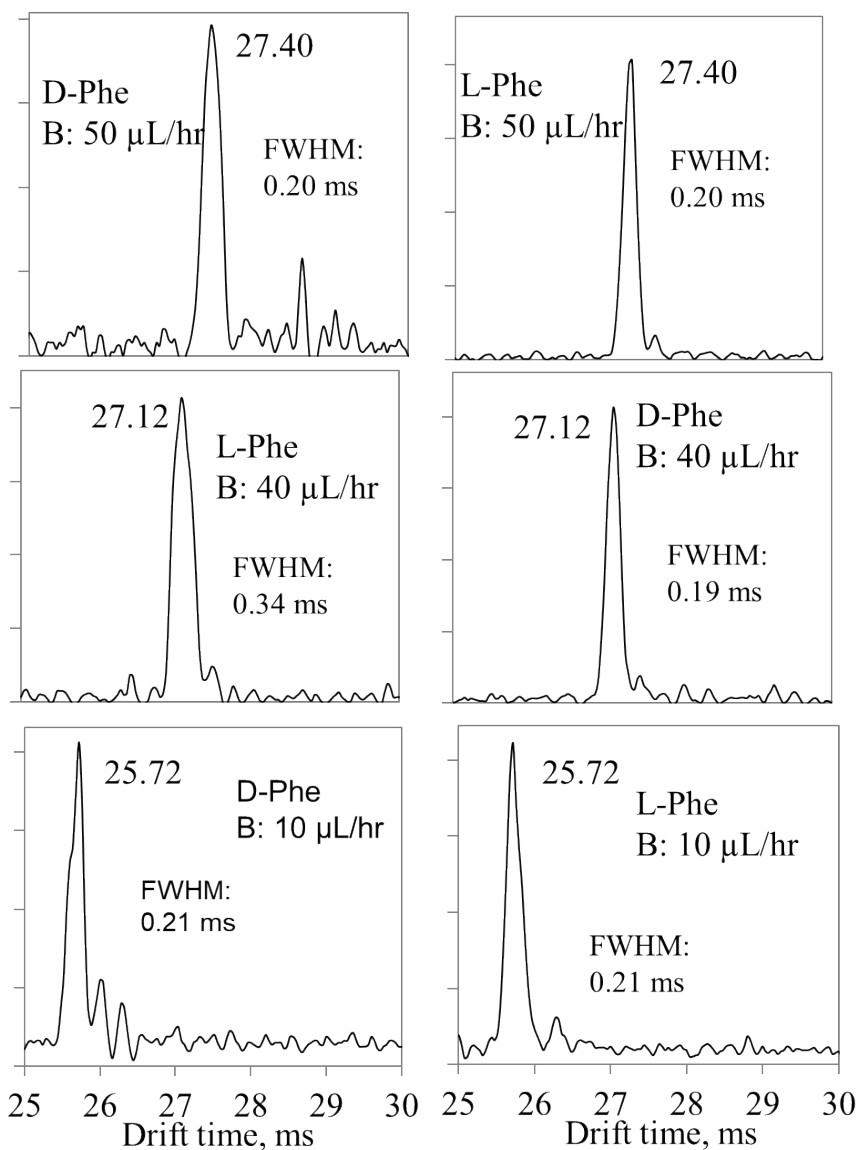


Figure S10. IMS spectra of the enantiomers D- and L- of phenylalanine (Phe) when 10, 40, and 50 $\mu\text{L/hr}$ of 2 butanol (B) was introduced in the buffer gas at 150°C. The same drift time was obtained for the enantiomers. FWHM: full-width at half-maximum. With these data, resolving power was calculated in Table S2.

Table S1. Review of seven studies cited by Nagy et al.⁸ about enantiomer separations. Any of these studies performed enantiomer separation by injecting only a chiral selector. Most of the studies separated enantiomers by forming chiral non-covalent diastereomeric complexes with other chiral molecules using transition metal cations.

Analytes	Method	Reference in Nagy's paper
l-glucose, d-glucose, l-allose, d-allose, d-gulose, d-galactose, and l-mannose	IMS-MS; monosaccharide enantiomers were separated by IMS-MS as metal-bound trimeric complexes with an amino acid or short amino acid chain in its L form acting as chiral reference compound	21
Isobaric dipeptides	IMS; crown ethers as shift reagents for non-enantiomeric isobaric dipeptides	22
Bile acids	Separation of Bile acid isomers by formation of cyclodextrin–bile acid host–guest inclusion complex	23
Amino acids	Amino acid enantiomers were separated by FAIMS as metal-bound trimeric complexes with another amino acid in its L form acting as chiral reference compound	24
Amino acids	TWIM-MS; cationisation with copper(II) and multimer formation with D-proline	25
Amino acids	FAIMS; Diastereomeric proton bound complexes were formed between enantiomers of amino acids (analytes) and <i>N-tert</i> -butoxycarbonyl- <i>O</i> -benzyl-l-serine	26
Non enantiomeric glycans	IMS-MS; glycan isomers complexed with different metal cations.	27
Isomeric carbohydrates	Determination of collisional cross sections for four groups of isomeric carbohydrates as their group I metal ion adducts	28

TWIM: traveling wave ion mobility spectrometry.

FAIMS: High-field asymmetric waveform ion mobility.

21. Gaye, M. M.; Nagy, G.; Clemmer, D. E.; Pohl, N. L., Multidimensional Analysis of 16 Glucose Isomers by Ion Mobility Spectrometry. *Anal Chem* 2016, 88, 2335-44.

<https://doi.org/10.1021/acs.analchem.5b04280>

22. Hilderbrand, A. E.; Myung, S.; Clemmer, D. E., Exploring Crown Ethers as Shift Reagents for Ion Mobility Spectrometry. *Anal. Chem.* 2006, 78, 6792-800.

10.1021/ac060439v

23. Chouinard, C. D.; Cruzeiro, V. c. W. D.; Roitberg, A. E.; Yost, R. A., Rapid Ion Mobility Separations of Bile Acid Isomers Using Cyclodextrin Adducts and Structures for Lossless Ion Manipulations. *J. Am. Soc. Mass Spectrom.* 2017, 28, 323-331.

<https://doi.org/10.1021/acs.analchem.8b02990>

24. Mie, A.; Jornten-Karlsson, M.; Axelsson, B. O.; Ray, A.; Reimann, C. T., Enantiomer Separation of Amino Acids by Complexation with Chiral Reference Compounds and High-Field Asymmetric Waveform Ion Mobility Spectrometry: Preliminary Results and Possible Limitations. *Anal. Chem.* 2007, 79, 2850-8. <https://doi.org/10.1021/ac0618627>
25. Domalain, V.; Hubert-Roux, M.; Tognetti, V.; Joubert, L.; Lange, C. M.; Rouden, J.; Afonso, C., Enantiomeric differentiation of aromatic amino acids using traveling wave ion mobility-mass spectrometry. *Chem. Sci.* 2014, 5, 3234-3239. <https://doi.org/10.1039/C4SC00443D>
26. Zhang, J. D.; Mohibul Kabir, K. M.; Lee, H. E.; Donald, W. A., Chiral recognition of amino acid enantiomers using high-definition differential ion mobility mass spectrometry. *Int. J. Mass Spectrom.* 2018, 428, 1-7. <https://doi.org/10.1016/j.ijms.2018.02.003>
- Zheng, X., Zhang, X., Schocker, N. S., Renslow, R. S., Orton, D. J., Khamsi, J., ... & Baker, E. S. (2017). Enhancing glycan isomer separations with metal ions and positive and negative polarity ion mobility spectrometry-mass spectrometry analyses. *Analytical and bioanalytical chemistry*, 409(2), 467-476.
28. Huang, Y.; Dodds, E. D., Ion Mobility Studies of Carbohydrates as Group I Adducts: Isomer Specific Collisional Cross Section Dependence on Metal Ion Radius. *Anal. Chem.* 2013, 85, 9728-35. <https://doi.org/10.1021/ac402133f>

Table S2. Resolving power of the IMS instrument for selected peaks of phenylalanine. The average resolving power was 116. These data were calculated with the IMS spectra in Figure S10. The time at which the spectra was taken is shown.

Cation	dt (ms)	B, $\mu\text{L/hr}$	FWHM	Rp	Time
D-Phe	27.40	50	0.30	91	16:41
L-Phe	27.40	50	0.20	137	16:49
L-Phe	27.12	40	0.34	80	15:39
D-Phe	27.12	40	0.19	143	15:44
D-Phe	25.72	10	0.21	122	12:03
L-Phe	25.72	10	0.21	122	12:11

dt: drift time; B: (S)-2-butanol flow rate; Rp: resolving power; FWHM: full-width at half-maximum. $10 \mu\text{L/hr} = 1.35 \text{ mmol m}^{-3}$

Table S3. Effect of chiral selector concentration on the mobilities of valinol enantiomers at 125 and 200°C (Figure 2). Here, 943- μ M solutions of D-valinol (\square), L-valinol (\diamond) and racemic mixtures (Δ) of valinol were analyzed at a buffer gas temperature of 125 °C and 200 °C. At 125°C, the enantiomers had the same drift time but the racemic mixture always yielded a single peak. At 200°C, the enantiomers had the same drift time because the valinol-(S)-2-butanol interaction decreased by the weak analyte-ligand bonds at high temperature and the difference in drift time between the enantiomers was too small. The drift times were statistically different ($P < 0.05$) when (S)-2-butanol was introduced at 125°C (bold text). The data for this table are plotted in Figure 2.

125°C		Drift time				
(S)-2-butanol mmol/m ⁻³	D-Valinol	L-Valinol	Average SD	n	dt-D/L- Valinol	n
0	20.21	20.21	0.04	5		
0.4	21.49	21.89	0.03	8	21.54	4
1.7	23.60	23.91	0.02	6	24.26	5
3.4	24.25	24.48	0.04	6		
5.1	24.63	24.79	0.05	8		
6.8	24.80	25.00	0.04	5		
200°C						
(S)-2-butanol mmol/m ⁻³	D-Valinol	L-Valinol	Average SD	n	dt-D/L- Valinol	n
0	17.20	17.21	0.03	4		
0.4	17.24	17.24	0.03	5	17.25	5
1.7	17.27	17.27	0.04	7	17.26	4
3.4	17.29	17.29	0.02	3		
5.1	17.30	17.29	0.03	4	17.30	3
6.8	17.30	17.30	0.02	6		

dt: drift time, ms; SD: standard deviations for D and L enantiomers; n: number of scans to obtain the average shown. Mobilities were measured for both enantiomers alternating between the R and S species.

Table S4. Drift times of valine enantiomers over an 8-hr period using (S)-2-butanol chiral selector (Figure S3). Solutions of D- valine (⊕), L- valine (⊖) and racemic mixtures of valine (Δ) at a 943-μM concentration were analyzed when 0.69 mmol m⁻³ (S)-2-butanol was introduced into the buffer gas at 150 °C. The drift times were different for both enantiomers (mean drift time separation of ~0.3 ms) but the racemic mixtures yielded only one peak, with a drift time similar to that of D-valine. Variations in drift time for the same enantiomer were caused mainly by changes in atmospheric pressure. The drift times of the enantiomers were statistically different (P<0.05).

Cation	RSD	dt	SD	n	Experiment sequence
L	0.103	19.42	0.02	4	1°
D	0.156	19.23	0.03	10	2°
L	0.102	19.53	0.02	7	3°
D	0.104	19.20	0.02	5	4°
D/L	0.208	19.26	0.04	3	5°
L	0.205	19.50	0.04	6	6°
D	0.207	19.30	0.04	6	7°
L	0.153	19.58	0.03	4	8°
D	0.149	19.42	0.03	5	9°
D/L	0.157	19.16	0.03	4	10°
L	0.206	19.41	0.04	5	11°
D	0.208	19.22	0.04	5	12°
L	0.103	19.38	0.02	5	13°

dt: drift time, ms; SD: standard deviation; n: number of scans to obtain the average shown.